# Coupled thermal and unloading-induced permeability of rock fractures

Tao Lin
*Tsinghua University, Beijing, China*

Zhihong Zhao
*Tsinghua University, Beijing, China*

Wen Meng
*Key Laboratory of Neotectonic Movement and Geohazard, Institute of Geomechanics, Chinese Academy of Geological Sciences, Beijing, China*

Xingguang Zhao
*CNNC Key Laboratory on Geological Disposal of High-level Radioactive Waste, Beijing Research Institute of Uranium Geology, Beijing, China*

ABSTRACT: The behavior of fluid flow through rock fractures is a critical issue in many subsurface rock engineering projects. Previous studies focused more on the permeability evolution of rock fractures under loading stage, while the change of fracture permeability under unloading stage is more consistent with the actual engineering excavation. To examine the unloading-induced changes in fracture permeability under different temperatures, we performed flow through tests on fractured core samples subjected to decreasing confining pressures and constant temperatures. The results show that the permeabilities of fractures under unloading confining pressure increase but decrease with increasing temperature because of fracture closure caused by asperity damage and thermal expansion. A coupled thermal-mechanical model considering asperity damage is used to explain the unloading-induced changes in fracture permeability. The coupled thermal-mechanical model properly predicts the experimental results.

*Keywords: Unloading, Permeability, Rock fracture, Temperature.*

## 1 INTRODUCTION

In the underground space creation or energy extraction, the continuous excavating inevitably breaks the original mechanical equilibrium state of rock masses, and the stress redistribution occurs in the surrounding (Florence et al. 2010). Fracture permeability is strongly dependent on stress paths, i.e., fracture permeability exhibits hysteretic behavior (Barton et al. 1985; Selvadurai 2015). Therefore, it is of practical significance to consider the effects of cyclic unloading on the seepage properties of fractured rocks.

Formation temperature increases with depth, and the increase of temperature will lead to the reduction of elastic modulus and compressive strength, as well as the increase of ductility in the post-peak zone (Huston et al. 2009), and the thermal expansion will cause the change of rock microstructure (Chaki et al. 2008). A number of tunnels are being or will be constructed in extremely warm or cold regions, e.g., the Blunkou-Gongger Hydropower Station in Xinjiang, China, is 82 °C, and the tunnel of Qirehataer Hydropower Station in Xinjiang, China, is up to 98 °C (Zeng et al., 2020; Zhao et al. 2021). The influence of temperature on permeability should be paid attention in the study.

The main aim of this study is to investigate the coupled thermal and unloading-induced permeability of rock fractures. We first conducted permeability tests on the artificial rock fractures under the unloading phase, during which the high temperatures up to 65 °C were kept. Second, a coupled thermal-mechanical model for fracture deformation was used to understand the underlying mechanisms of coupled thermal and unloading-induced permeability.

## 2 METHODOLOGY

The main experimental procedure including sample preparation and coupled thermal-mechanical model for unloading deformation are presented here.

### *2.1 Experimental procedure*

Core samples were collected from the boreholes (depth of about 620 m) at the Layue tunnel construction site in Nyingchi, Tibet, China and axially split to produce an artificial fracture between the two semicircular halves with Brazil splitting method. Before and after the permeability test, we scanned the fracture morphology with a three-dimensional (3D) blue light scanner (OKIO-5M, TENYOUN), which could be used in subsequent numerical calculations. ROCK 600-50 VHT high temperature triaxial rheological test system was used to perform permeability test subjected to confining pressures and temperatures (see Figure 1).

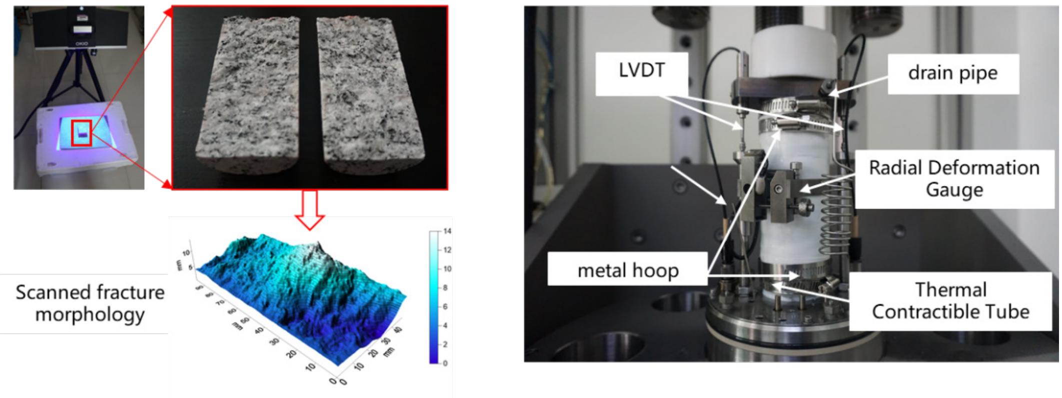

Figure 1. Scanned fracture morphology and prepared sample in test system.

In the permeability tests, the maximum axial stresses for fractured samples were 60 MPa and the maximum confining stresses were set as 60 MPa to simulate the conditions of depth in 2000 m, which are the potential risky sections of the Layue tunnel. The target temperature is 25-65 °C according to the site engineering geological data. The main experimental procedure is as follows: 1) Place the samples into the confining chamber; 2) Apply the designed confining pressure and temperature conditions and keep it for 2 h to ensure the sample is heated to specific temperature; 3) Perform quasi-stationary flow permeability test; 4) Repeat the second and third steps. The steady-state method was used to measure the sample permeability, and the widely used parallel plates was adopted to measure the permeability of the fractured samples as the cubic law (Witherspoon et al. 1980)

$$q = -\frac{\mathrm{w} e_h^3}{12\mu} \cdot \frac{dp}{dx} \tag{1}$$

where $p$ is the water pressure, $x$ is the fracture axis, $\mu$ is the dynamic viscosity of the fluid ($8.89\times10^{-4}$, $5.94\times10^{-4}$, $4.31\times10^{-4}$ Pa·s under the temperatures of 25, 45, and 65 °C, respectively.), $q$ is the volumetric flow rate, $e_h$ is the fracture hydraulic aperture, $w$ is the width of the fracture (equals to the diameter of the core sample).

## *2.2 Coupled thermal-mechanical model for unloading deformation*

Based on the fracture deformation model established by Hopkins (1991), Pyrak-Nolte and Morris (2000), Peng et al. (2020), a fracture can be regarded as two half-spaces separated by a large number of cylindrical asperities with the same radius but varying height, which can be calculated from topography data scanned by the 3D blue light scanner. The average displacements ($w_{ij}$) of the half-spaces at asperity $i$ caused by asperity $j$ and asperity $i$ itself are as follows (Hopkins 1990):

$$w_{ij} = f_j \frac{8(1-v^2)}{\pi^2 E a^2} \iint_{S_i} \left( \int_0^{\pi/2} \sqrt{1-\left(\frac{a^2}{r^2}\right) sin^2\theta d\theta} - \left(1 - \frac{a^2}{r^2}\right) \int_0^{\pi/2} \frac{d\theta}{\sqrt{1-\left(\frac{a^2}{r^2}\right) sin^2\theta}} \right) r\, drd\theta \tag{2}$$

$$w_{ii} = f_j \frac{8(1-v^2)}{\pi^2 E a^2} \iint_{S_i} \left( \int_0^{\pi/2} \sqrt{1-\left(\frac{a^2}{r^2}\right) sin^2\theta d\theta} \right) r\, drd\theta \tag{3}$$

where $S_i$ is the area of asperity $i$, $E$ is Young's modulus, $v$ is Poisson's ratio, $a$ is the asperity radius, $r$ and $\theta$ are polar coordinates. The total displacement at asperity $i$ from all of the asperities that are in contact can be determined.

$$W_i = \sum_{j \in c} w_{ij} \tag{4}$$

In this study, the change in asperity height and Young's modulus induced by temperature in the absence of stress are (Peng et al. 2020).

$$L_i = (1 + \alpha \Delta \mathrm{T}) L_i^0 \tag{5}$$

$$E = (1 + \beta \Delta \mathrm{T}) \mathrm{E}_0 \tag{6}$$

where $\alpha$ is the coefficient of thermal expansion, $\beta$ is the coefficient of Young's modulus variation with temperature, $E_0$ is the Young's modulus at the room temperature, and $\Delta$T is the change in temperature. $L^0_i$ is the original unstressed length of asperity i, which is defined as (Peng et al. 2020):

$$L_i^0 = \mathrm{D}_0 - \mathrm{A}_i \tag{7}$$

where $D_0$ is the original distance between the two half-spaces, $A_i$ is aperture between two half-spaces. After the cylindrical asperities get heated or loaded, the height will deform as elastic-perfectly plastic materials with irrecoverable residual deformation. The residual deformation ($\Delta L_{e,m}$) is proportional to the original deformation ($\Delta L_e$ ) when unloading (Peng et al. 2020):

$$\Delta L_{e,m} = \xi \Delta L_e \tag{8}$$

where ξ is a proportionality factor. Combining Eqs. (2-8), the asperity heights and apertures during unloading under constant temperatures is calculated. Table 1 shows the numerical parameters of the thermal-mechanical model.

Table 1. Parameters used in the thermal-mechanical model.

| Coefficients | Value | Unit | Reference |
|---|---|---|---|
| Asperity radius (a) | 0.5 | mm | This study |
| Original distance between the two half-spaces ($D_0$) | 10 | mm | This study |
| Yield stress of the asperity ($\sigma_o$) | 140 | MPa | This study |
| Young's modulus at the reference temperature ($E_0$) | 40 | GPa | This study |
| Poisson's ratio (ν) | 0.35 | - | This study |
| Coefficient of thermal expansion (α) | $3\times10^{-6}$ | - | This study |
| Coefficient of Young's modulus (β) | 0.0015 | - | Wang et al. (2019) |
| ξ | 0.15 | - | |

## 3 RESULTS

The coupled thermal-mechanical model was applied to investigate the permeability variation during thermal-unloading process, and the surface morphology of fracture, or the asperities in the model could clearly display the damaged zones in the test, which could be applied to further investigate the influence of coupled thermal and loading-unloading process, including the unloading hysteresis phenomena.

### 3.1 *Effect of unloading on rock fracture permeability*

Figure 2 shows the pressure conditions and normalized permeability for experiment and calculation evolution of permeability. The fracture permeability increased with decreasing confining pressures. At room temperature of 25 °C, the permeability of the sample is $0.53\times10^{-9}$ $m^2$ at the maximum confining pressure, and became$2.75\times10^{-9}$ $m^2$ at confining pressure of 10 MPa, i.e., increased by 5.17 times. Considering the different temperature, the permeability decreased with increasing temperatures. Note that this phenomenon may also include the effect of cycling unloading, which was not distinguished in the test. In addition, creep may also lead to the reduction of permeability, which can be further explained in the change of surface morphology of the proposed thermo-mechanical coupling model.

### 3.2 *Coupled thermal-mechanical model*

A central area of the sample with a size of 45 mm × 90 mm is selected to avoid boundary effect. The asperity radius (a) is set at 0.5 mm to balance calculation accuracy and efficiency, so there are 4050 cylindrical asperities in the model. The parameters in the coupled thermal-mechanical model are presented in Table 1, and most are from the axial compression experiments with the same kinds of sample drilled from the project. Figure 2 gives the comparison about the fracture aperture during the experiments. The sample shows a fairly good agreement. The fitness between experiment and simulate results is likely related to 1) The experiment results are hydraulic aperture but the simulation is mechanical aperture, 2) During the experiment, long-time resisting the high confining compression may cause the creep in the sample, so the calculated results tend to be higher than the experiment results. Even though, the variation tendency of aperture with confining pressure and temperature is same.

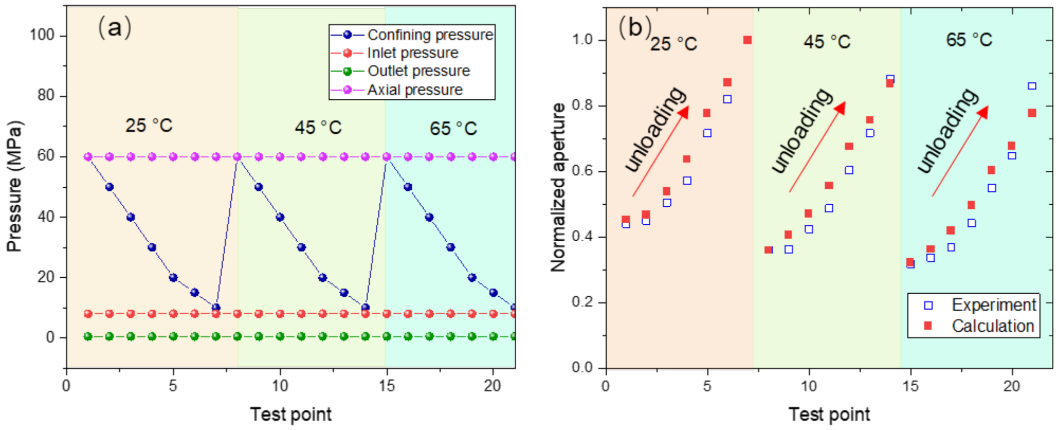

Figure 2. Pressure conditions (a) and normalized permeability for experiment and calculation (b).

Loading-unloading caused hysteresis in the fracture permeability has been reported in literature (Huang et al. 2021; Wang et al. 2021), with proposed coupled thermal-mechanical model, the thermal-loading-unloading process was calculated. The recovery rate is defined as the ratio of the unloaded permeability to the permeability during loading under the same temperature and pressure. Figure 3 displays the loading-unloading process for normalized aperture and recovery rate with different pressure and temperature. With the increase of cyclic loading times, the normalized aperture decreases the most in the first cycle, and gradually becomes stable in the following cycles. This is because the convex asperities have irrecoverable deformation or damage, making the surface of the fracture tend to be flat. This is similar to the results of other research in the experimental study (Honglian et al. 2018; Long et al. 2019). The curve of recovery rate also shows the same rule. With the subsequent loading process, the permeability of the unloading process is close to the loading process.

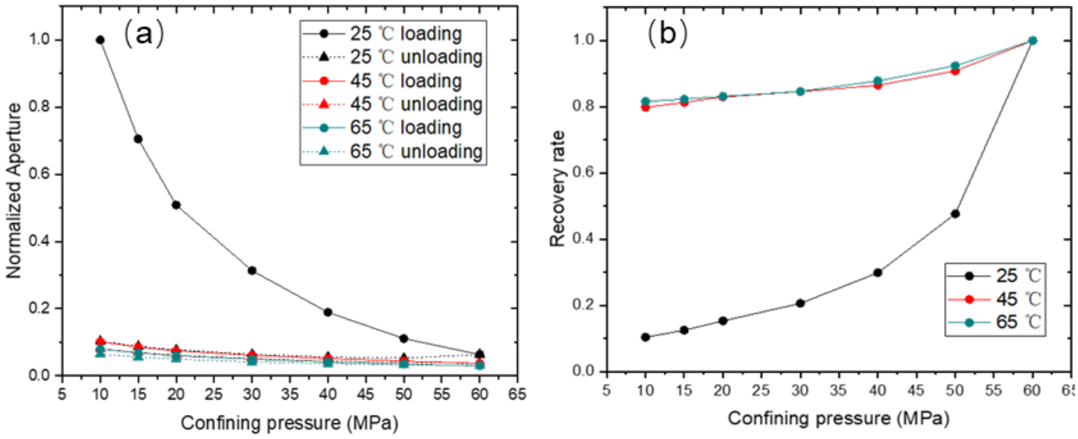

Figure 3. Loading-unloading process for normalized aperture (a) and recovery rate with different pressure and temperature (b).

# 4 CONCLUSIONS

This study investigates coupled thermal and unloading-induced permeability of rock facture. A permeability test was performed on a cylindrical Layue granite sample and a coupled thermal-mechanical model for fracture deformation during unloading process was derived. The permeabilities of fractures under unloading confining pressure will increase but decrease with increasing temperature because of fracture closure caused by asperity damage and thermal expansion. A coupled thermal-mechanical model can consider mechanical and thermal damage and properly predict the experimental results.

# ACKNOWLEDGEMENT

This work is supported by the jointly supported by the National Natural Science Foundation of China (U2067203, 51739006).

# REFERENCES

Barton N, Bandis S, Bakhtar K .1985. Strength, deformation and conductivity coupling of rock joints. *International Journal of Rock Mechanics & Mining Sciences & Geomechanics Abstracts*. 22, pp. 121–140. DOI：10.1016/0148-9062(85)93227-9

Chaki S，Takarli M，Agbodjan W P. 2008. Influence of thermal damage on physical properties of a granite rock：porosity，permeability and ultrasonic wave evolutions. *Construction and Building Materials*，22, pp.1456–1461

Fan L, Liu S. 2019. Evaluation of permeability damage for stressed coal with cyclic loading: An experimental study. *International Journal of Coal Geology*, 216. DOI：10.1016/j.coal.2019.103338

Florence, Nicollin, Dominique, et al. 2010. Anisotropy of electrical conductivity of the excavation damaged zone in the Mont Terri Underground Rock Laboratory. *Geophysical Journal International*, 181, pp. 303-320. DOI：10.1111/j.1365-246X.2010.04517.x

Hopkins D. 1990. *The effect of surface roughness on joint stiffness, aperture, and acoustic wave propagation*. PhD Thesis, The University of California at Berkeley, USA.

Hudson J A，Harrison J P. 2009. Engineering rock mechanics. Translated by FENG Xiating. Beijing：Science Press.81.(in Chinese)

Li H, Tang J, Lu Y, et al. 2018. Experimental Measurements of Shale Fracture Conductivity Under Cyclic Loading. *Arabian journal for science and engineering*. DOI. 10.1007/s13369-017-3032-y

Peng H, Zhao Z, Chen W, Chen Y, Fang J, Li B. 2020. Thermal effect on permeability in a single granite fracture: Experiment and theoretical model. *International Journal of Rock Mechanics and Mining Sciences*, 131, pp. 104358. DOI：10.1016/j.ijrmms.2020.104358

Pyrak-Nolte LJ, Morris JP. 2000. Single fractures under normal stress: the relation between fracture specific stiffness and fluid flow. *International Journal of Rock Mechanics and Mining Sciences* 37, pp. 245-262. DOI：10.1016/S1365-1609(99)00104-5

Selvadurai APS. 2015. Normal stress-induced permeability hysteresis of a fracture in a granite cylinder. *Geofluids* 15, pp. 37-47. DOI：10.1111/gfl.12107

Witherspoon PA, Wang JSY, Iwai K, Gale JE. 1980. Validity of cubic law for fluid flow in a deformable rock fracture. *Water Resources Research* 16, pp. 1016-1024. DOI：10.1029/WR016i006p01016

Zeng Y, Tao L, Ye X, et al. 2020. Temperature reduction for extra-long railway tunnel with high geotemperature by longitudinal ventilation. *Tunnelling and Underground Space Technology* 99, pp. 103381. DOI：10.1016/j.tust.2020.103381

Zhao Z, Xu H, Liu G, Liu F, Wang G. 2021. A robust numerical method for modeling ventilation through long tunnels in high temperature regions based on 1D pipe model. *Tunnelling and Underground Space Technology* 115, pp. 104050. DOI：10.1016/j.tust.2021.104050